

COMPUTER SIMULATION FOR CURRENT DENSITY IN PN-SILICON SOLAR CELLS

FATHI Y. R. EL FAITURI and ALI Y. DARKWI

University of Garyounis, Benghazi-Libya

E-mail: Fathi_ff2002@yahoo.com

E-mail: alidarkwi@yahoo.com

Abstract. Numerical analysis of electric field and potential profile in depletion layer of an abrupt Si p-n junction solar cells has been made by solving Poisson's equation. The variation of depletion layer as well as the electrostatic potential and electric field with forward bias voltage were also analyzed. The transport and continuity equations for the charge carrier were solved numerically to obtain the current density. The evaluated current density considered both the diffusion in neutral regions of (p and n) and drift within depletion layer. The influence of lifetime and surface recombination speed of charge carries in the efficiency of the cell were also discussed.

Key words: pn junction, electron and hole life time, surface recombination speed

1. Introduction

The conversion of sunlight directly to electric power has been dominated by solid state junction devices. The junction between different material can set up an internal electric field, which is responsible for separation of charge pairs (electron and hole) that are generated by incident photons. The distribution of electric field in the depletion layer can be obtained by solution of Poisson's equation. Although this equation does not appear to have an analytical solution, many articles (Green, 1982; Pierret, 1996; Zambuto, 1989) deal with an analytical treatment, which allows an easy interpretation of physical results and direct control on the involved parameters. A limitation of analytical models lays in the need of simplified assumption on the physics of the device, which may only be accepted in order to reduce the complexity in the calculation. Numerical treatment offers a deeper comprehension of the structure, achieving a complete control on the various parameters and defining their role in the device operation. A very important contribution in the numerical analysis of electrostatic potential and electric field in a depletion layer of linearly-graded p-n junction has been introduced by Kennedy and O'Brien (1967). In their analysis, the space-charge density modifications arise from impurities as well as from free charge of electrons and holes. In particular, our analysis is based on the numerical solution of Poisson's equation in the depletion layer of an abrupt Si p-n junction. The space-charge density ρ involved in the calculation considers both the charge due to impurities and free charge of electrons and holes, however, some articles consider only the charge due to impurities (Green, 1982; Tsaur *et al.*, 1972). The calculation has been done for equilibrium (V bias =0) and under forward bias voltage. The aim of this calculation is focused on an accurate determination of space charge density and the behavior of depletion layer under

bias voltage. A numerical model has been developed to find the current density. Based on physical consideration on minority carriers, the transport and continuity equations were solved numerically. Flexibility of the model lies in the capability of obtaining the carrier distribution and hence, the current density varying with material parameters or structure parameters. In this analysis we have tried to show how the efficiency of the cell can be enhanced by changing the parameters involved in the calculation.

2. Electric Field Within Depletion Layer of An Abrupt p-n Junction

The distribution of electric field within the depletion layer can be analyzed by solving Poisson’s equation

$$\frac{d^2\phi}{dx^2} = -\frac{1}{\epsilon}\rho(x, \phi) \tag{1}$$

Where ϕ is the electric potential, ϵ is dielectric constant, ρ is the space charge density, and x is the depth in the depletion layer. The space charge density in the depletion layer is given by

$$\rho = q [N_d(x) - N_a(x) + p(\phi) - n(\phi)] \tag{2}$$

where $p(\phi)$ and $n(\phi)$ are the concentration of free charge of holes and electrons respectively, $N_d(x)$ and $N_a(x)$ are the concentration of ionized donors and acceptors(Sze, 1981).

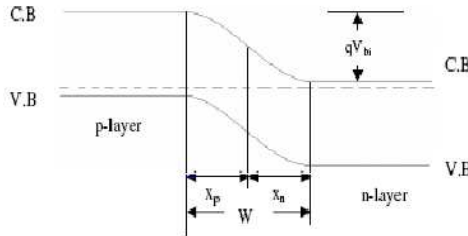


Fig. 1. The pn junction at equilibrium.

Within the depletion layer, Eq.(1) was solved numerically. The left side of the equation can be approximated by

$$\frac{\phi_{i-1} - 2\phi_i + \phi_{i+1}}{h^2} - err(h) = -\frac{\rho(x_i, \phi_i)}{\epsilon} \tag{3}$$

Where h is an increment ($h = x_{i+1} - x_i$) and the part $err(h)$ is the local error. When h is very small, this term can be neglected. Hence, eq.(3) becomes

$$\phi_{i-1} - 2\phi_i + \phi_{i+1} + \frac{h^2\rho(x, \phi)}{\epsilon} = 0 \tag{4}$$

Where $i = 1, \dots, N$.

With a proper physical boundary conditions (EL Faituri, 2004), the above equation was solved by iteration method. The space-charge density, electrostatic potential and electric field are shown in the following figures. For an abrupt p-n junction, the doping profile of the impurity is assumed to be uniform throughout each semiconductor (p and n) up to the junction. Within depletion layer, the doping profile is shown in Fig. 2 curve (a). While the free negative $n(\phi)$ and positive $p(\phi)$ charge density within depletion layer which tails off as one proceed toward the junction is illustrated in curve(b) and (c) respectively. Since the density of free charges $n(\phi)$ and $p(\phi)$ were low comparing to the density of donor N_d and acceptor N_a , the shape of net charge density is overruled by impurities (N_a and N_d) as shown in curve (d); however, the contribution of free charges become clear in reducing the space-charge density. The corresponding electrostatic potential and electric field is shown in curve (e) and (f) respectively. The analysis was carried out under equilibrium conduction (bias voltage $V=0$). The continuity of electrostatic potential and electric field at $x = 0$ justifies the condition of charge neutrality (Zambuto, 1989), for which $N_a x_p = N_d x_n$. Within the depletion layer, the electric field is negative, has maximum value at $x=0$ and exhibits a linear variation with position. The negative profile of the electric field simply originates from the choice of the boundary condition in one dimension for which the electric field is pointed in the negative x -direction, while the linear variation of electric field with position is due to charge distribution. Since there is no charge outside the depletion layer, the electric field becomes zero in the neutral region of n and p.

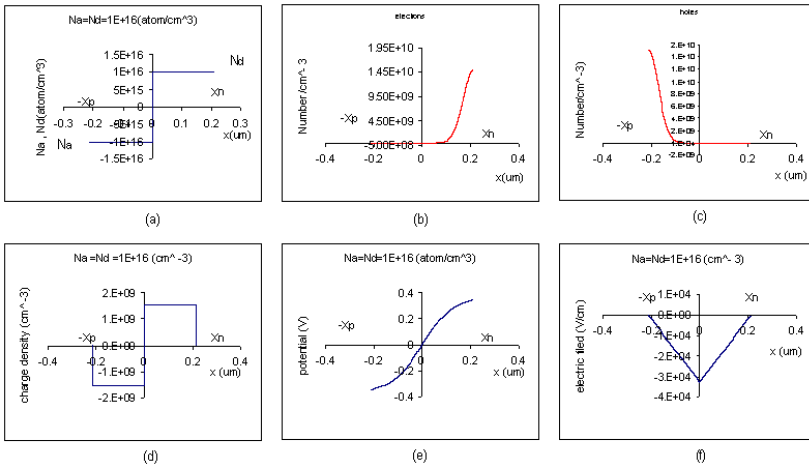


Fig. 2. Curves for an abrupt p-n junction in silicon at 300 K, Curve (a) shows the density of donor ($N_d = 10^{16} \text{ cm}^{-3}$) and acceptor ($N_a = 10^{16} \text{ cm}^{-3}$) atoms within the depletion layer as a function of x , curves (b) and (c) show the density of free negative charge ($n(x)$) and positive ($p(x)$) within the depletion layer; Curve (d) shows the net charge density $\rho(x)$ within the depletion layer related to curves (a),(b)and (c); Curve (e) shows the electric potential within the depletion layer as a function of x ; curve (f) shows the electric field within the depletion layer as a function of x .

As a matter of fact, the solar cell operates in forward bias voltage, therefore we are particularly interested in how the electrostatic variables (potential and field)

could change under this biasing. In forward bias case, the barrier between p-and n-side is reduced to the relation $V_{bi} - V$ where $V > 0$. The lower barrier permits a large portion of majority carriers to cross the junction into the adjacent semiconductor, where they now become minority. The pileup of minority carriers in the immediate vicinity of the depletion layer results in concentration gradient, which causes diffusion of the carriers away from the junction toward a quasineutral region, where they recombine with the majority. Hence, the diffusion causes a reduction of charge along the two sides of the junction (Zambuto, 1989). Therefore, the depletion layer becomes narrow, the electrostatic potential and electric field decrease everywhere inside the depletion layer. Fig.3. shows, the electrostatic potential and electric field profiles within the depletion layer at forward bias voltage 0.2 and 0.4 volt.

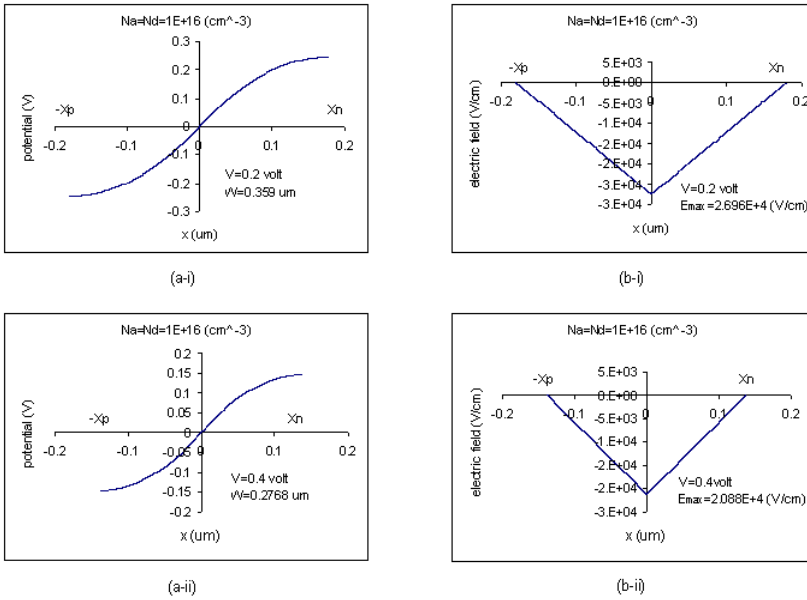


Fig. 3. Curves for an abrupt p-n junction in silicon at 300 K, under forward bias voltage. Density of donor and acceptor atoms is $N_d = 10^{16}$ and $N_a = 10^{16}$ respectively: (a) the electric potential within the depletion layer as a function of x , (b) the electric field within the depletion layer as a function of x . Where: W , is the width of the depletion layer, E_{\max} , is the maximum value of the electric field and V is the forward bias voltage.

3. Analysis of Current Density

The current density was obtained by the solution of the electron and hole continuity equations

$$-\frac{1}{q} \frac{dJ_n(x)}{dx} = G(x) - R(x) \tag{5}$$

$$\frac{1}{q} \frac{dJ_p(x)}{dx} = G(x) - R(x) \quad (6)$$

where

$$J_n = q\mu_n n(x)E(x) + qD_n \frac{dn(x)}{dx} \quad (7)$$

and

$$J_p = q\mu_p p(x)E(x) - qD_p \frac{dp(x)}{dx} \quad (8)$$

are the electron and hole conduction current densities. $G(x)$ is the generation rate, $R(x)$ is the recombination rate, μ_n and μ_p are the mobility of free electrons and holes, D_n and D_p are the diffusion coefficients of electrons and holes respectively.

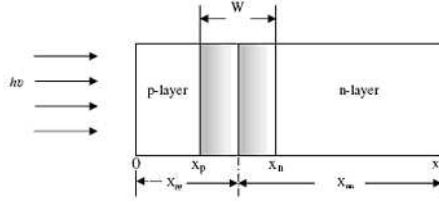


Fig. 4. p-n junction solar cell illuminated from p-side.

The generation rate $G(x)$ of charge carriers in the semiconductor layer at the depth x is given by;

$$G(x) = \int_0^{\lambda_{max}} [1 - R(\lambda)] \alpha(\lambda) N_{ph}(\lambda) e^{-\alpha(\lambda)x} d\lambda \quad (9)$$

where $\alpha(\lambda)$ is the absorption coefficient, $N_{ph}(\lambda)$ is the incident photon flux, $R(\lambda)$ is the reflection coefficient at front surface. λ_{max} is the maximum wavelength determined by the condition that, each photon with energy $h\nu \geq E_{gap}$ could generate electron-hole pairs. The recombination rate $R(x)$ is described by the lifetime of electrons (τ_n) and holes (τ_p) as follows (Fonash, 1981);

$$R(x)_n = \frac{\Delta n(x)}{\tau_n} \quad (10)$$

$$R(x)_p = \frac{\Delta p(x)}{\tau_p} \quad (11)$$

where $\Delta n(x)$ and $\Delta p(x)$ are the excess electron and hole concentrations respectively. The electric field within the neutral region of the p- and n layer is zero, hence, using equations (7) and (8), the equations (5) and (6) can be reduced into second-order differential equations of the form

$$D_n \frac{d^2 \Delta n(x)}{dx^2} - \frac{\Delta n(x)}{\tau_n} + G(x) = 0 \quad (12)$$

$$D_p \frac{d^2 \Delta p(x)}{dx^2} - \frac{\Delta p(x)}{\tau_p} + G(x) = 0 \tag{13}$$

Eqs.(12) and (13) are iteratively solved with appropriate boundary conditions (Sze, 1981; Donald, 1992). The current densities due to diffusion of charge carriers are analyzed using (Sze, 1981).

$$J_n = qD_n \frac{d\Delta n}{dx} \Big|_{x=x_p} \tag{14}$$

and

$$J_p = -qD_p \frac{d\Delta p}{dx} \Big|_{x=x_n} \tag{15}$$

Within the depletion layer, the electric field is generally high. We assume that, the photogenerated carriers are accelerated out of the depletion layer before they can recombine. Thus, the current density due to depletion layer is

$$J_{dep} = q \int_0^{\lambda_{max}} [1 - R(\lambda)] N_{ph}(\lambda) e^{-\alpha(\lambda)x_p} [1 - e^{-\alpha(\lambda)W}] d\lambda \tag{16}$$

The total photocurrent density is then

$$J_{ph} = J_n + J_p + J_{dep} \tag{17}$$

and the total current density

$$J(V) = J_{ph} - J_{dark} \tag{18}$$

where $J_{dark} = J_0 [e^{\frac{qV}{kT}} - 1]$. J_0 is the saturation current density.

4. Interpretation of Numerical Results

Figure 5 presents the numerical result on current density profiles as a function of charge carriers lifetime. Curves in panel (a) show the current density calculated for two solar cells with different hole lifetime while electron lifetime is kept at $\tau_n = 10^{-6}$ sec. The short circuit current density (J_{sc}) and efficiency (E_{ffi}) are reduced as the lifetime decreases. In fact, when the charge carrier lifetime decreases, the diffusion length ($L = \sqrt{D\tau}$) becomes small and hence a few carriers can contribute in the diffusion process. This causes reduction in short circuit current density. The curves in panel (b) was obtained by keeping the hole lifetime fixed at $\tau_p = 10^{-6}$ sec while changing the electron lifetime. We can see that both (J_{sc}) and (E_{ffi}) present an appreciable reduction which imply the same conclusion pointed above.

Figure 6 shows the current density characteristics for a solar cell as a function of surface recombination speed of charge carrier. Curves in panel (a) and (b) show the current density when varying then electron surface recombination speed (S_n) keeping the hole surface recombination speed (S_p) unchanged. As the electron surface recombination speed decreases, the short circuit current (J_{sc}) and the efficiency (E_{ffi}) increase in agreement with the result obtained by (Yasutake *et al.*, 1994).

TABLE I
parameters used for numerical calculations

Parameter	Value
T	Temperature, 300K
ϵ_s	Dielectric constant for silicon, $1.0610 \cdot 10^{-10} \text{ Fm}^{-1}$
D_n	Diffusion coefficient of electrons, $D_n=34.91(\text{cm}^2/\text{s})$
D_p	Diffusion coefficient of holes, $D_p=12.41(\text{cm}^2/\text{s})$
X_{pp}	Width of p-layer at zero bias voltage, $5 \mu \text{ m}$.
W	Width of depletion layer at zero bias voltage, $0.0201 \mu \text{ m}$
X_{nn}	Width of n-layer at zero bias voltage, $245 \mu \text{ m}$
$\alpha(\lambda)$	Absorption coefficient of Si (Aspnes <i>et al.</i> , 1983)
$R(\lambda)$	Reflection coefficient at the front surface (EL Faituri, 2004)
$N_{ph}(\lambda)$	Incident Photon flux for AM1, ($100 \text{ mW}/\text{cm}^2$) (Chopra and Das, 1983)
τ_n, τ_p	Lifetime of electrons and holes respectively, (from 10^{-6} to 5×10^{-4} sec) (Duffie and Beckman, 1974)
S_n, S_p	Surface recombination speed for electrons and holes respectively ($10^2, 10^5 \text{ cm}/\text{sec}$) (Datta <i>et al.</i> , 1994)

Curves in panel (c) and (d) are obtained by keeping the electron surface recombination speed constant and changing the hole surface recombination speed. For the case of long base layer (n-layer), there is no big change in (J_{sc}) and (E_{ffi}). This because, the rate of generation and collection of charge carriers remain the same at the back of the base layer. However, when the base layer becomes short, the distribution of generated charge carriers becomes high (EL Faituri, 2004). For short base layers the (J_{sc}) and (E_{ffi}) become high as the surface recombination speed decreases. The result corresponds to what indicated in some articles (Datta *et al.*, 1994; Yasutake *et al.*, 1994), for which the efficiency of thin silicon solar cell increases while (S_n) and (S_p) become small.

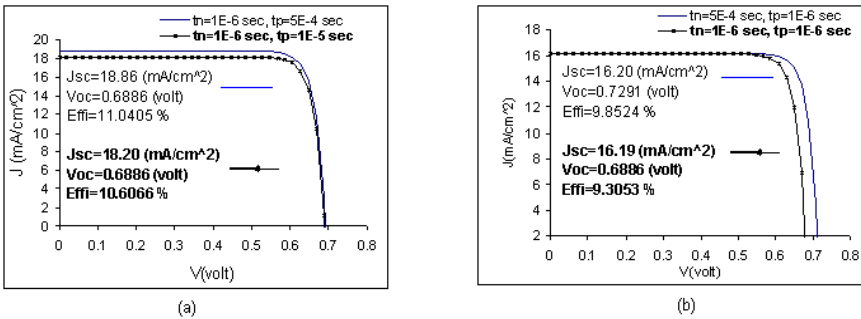


Fig. 5. Calculated J-V characteristics as a parameter of lifetime. Curves in panel (a) consider cells with the same electron lifetime but different hole lifetime, curves (b) represent the inverse situation, same τ_p but different τ_n .

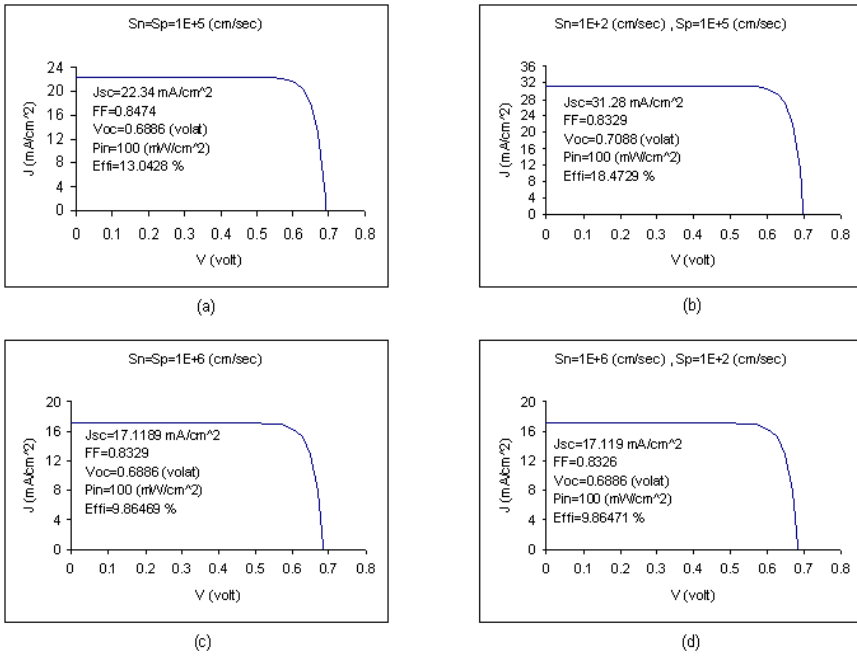


Fig. 6. Calculated J-V characteristics as a parameter of surface recombination speed. Curves in panels (a) and (b) consider cells with the same hole surface recombination speed but different electron surface recombination speed, curves (c) and (d) are obtained for the inverse situation, same S_n but different S_p .

5. Conclusion

In this paper, an accurate analysis of charge density in the depletion layer has been considered. It has been shown that, the density of charge within the depletion layer decreases when free charges (electrons and holes) are involved in the calculations. Because of the low density of free charges compared to the charge density due to impurities, the shape of space-charge density is overruled by impurities. From J-V characteristics, the effect of surface recombination speed of charge carriers, shows that, the efficiency increases as the surface recombination speed decreases. Therefore, for good solar cell fabrication, one can chose materials that have low surface recombination speed in the front and back contact of the cell.

References

- Aspnes, D. E. and Studna, A. A.: 1983, *Physical Review B*, **27**, 985
- Chopra, K. L. and Das, S. R.: 1983, *Thin Film Solar Cells*, Plenum press, New York, P. 508
- Datta, S. K., Mukhopadhyay, K., Pal, P. K., Saha, H.: 1994, *Solar Energy Materials and Solar Cells*, **33**, 483
- Duffie, J. A. and Beckman, W. A.: 1974, *Solar Energy Processes*, John Wiley and Sons, Inc.
- EL Faituri, F. Y.: 2004, Msc. Thesis, University of Garyounis.
- Fonash, S. J.: 1981, *Solar Cell Device Physics*, Academic press, Inc, P. 150
- Green, M. A.: 1982, *Solar Cells*, Prentice-Hall, Inc., Englewood Cliffs, New Jersey, P. 66

- Kennedy, D. P., O'Brien, R. R.: 1967, *IBM Journal of Research and Development* **11**, no.3, 252
- Donald A. N.: 1992, *Semiconductor Physics and Devices*, IRWIN, Inc, P. 247
- Pierret, R. F.: 1996, *Semiconductor Device Fundamentals*, Addison-Wiley Publishing Company, Inc.
- Sze, S. M. : 1981, *Physics of Semiconductor Devices*, by John Wiley and Sons, Inc.
- Tsaur, S. C., Milnes, A. G., Sahai, R. and Feucht, D. L.: 1972, in *Symposium on GaAs. Inst. of Phys. and Phys. Soc., London.*, 156
- Yasutake, K., Chen, Z., Pang, S. K., and Rohatgi, A.: 1994, *J. Appl. Phys.*, **75**, (4), 2048
- Zambuto, M.: 1989, *Semiconductor Devices*, Mc Graw-Hill Book Company, P. 183